

**Single-photon emission from the natural quantum dots in the InAs/GaAs wetting layer**T. Kazimierczuk,<sup>1</sup> A. Golnik,<sup>1</sup> P. Kossacki,<sup>1</sup> J. A. Gaj,<sup>1,\*</sup> Z. R. Wasilewski,<sup>2</sup> and A. Babiński<sup>1,†</sup><sup>1</sup>*Institute of Experimental Physics, Faculty of Physics, University of Warsaw, ul. Hoża 69, PL-00-681 Warszawa, Poland*<sup>2</sup>*Institute for Microstructural Sciences, National Research Council, Ottawa, Ontario, Canada K1A 0R6*

(Received 17 June 2011; published 26 September 2011)

A time-resolved microphotoluminescence study is presented for quantum dots that are formed in the InAs/GaAs wetting layer. These dots are due to fluctuations of In composition in the wetting layer. They show spectrally sharp luminescence lines with a low spatial density. We identify lines related to neutral exciton and biexciton as well as trions. Exciton emission antibunching [second-order correlation value of  $g^{(2)}(0) = 0.16$ ] and a biexciton-exciton emission cascade prove nonclassical emission from the dots and confirm their potential as single-photon sources.

DOI: [10.1103/PhysRevB.84.115325](https://doi.org/10.1103/PhysRevB.84.115325)

PACS number(s): 78.55.Cr, 78.66.Fd, 78.67.Hc

**I. INTRODUCTION**

Quantum confinement of carriers in semiconductor quantum dots (QDs) leads to numerous effects of fundamental character. This makes them objects of intense study (for a review, see Ref. 1). The research is driven by both scientific curiosity and applications, e.g., in optical quantum devices based on single-photon emission.<sup>2</sup> Such photoluminescence relies on cascade process with spectrally distributed multiexcitonic emissions and the recombination of a single exciton as the final step of the sequence. Although the single-photon emission has been observed in several physical systems, its QD realization promises an easy incorporation in optoelectronic semiconductor devices. The single-photon emission in QDs has been shown in several systems, including InAs/GaAs self-assembled QDs<sup>2</sup>, CdSe/Zn(S,Se),<sup>3</sup> CdTe/ZnTe QDs,<sup>4,5</sup> and *naturally* occurring QDs with confinement resulting from monolayer width fluctuations of a thin GaAs/GaAlAs<sup>6</sup> quantum well. In this work we investigate a potential of *natural* QDs present in a wetting layer (WLQDs), which accompanies InAs/GaAs self-assembled QDs<sup>7</sup> as single-photon emitters. We report on the correlation spectroscopy of excitonic complexes confined in the dots. Experimental evidence of the radiative cascade between the biexcitonic and excitonic emissions in the WLQDs is presented. Charged exciton-neutral exciton cross-correlation experiments confirm the attribution of the excitons to the same WLQD. The radiative lifetimes of the excitons have been measured and have been found to be of the same order as values usually observed in InAs/GaAs self-assembled QDs. This paper is organized as follows. Information on the investigated sample and experimental setup is provided in Sec. II. Results of microphotoluminescence ( $\mu$ PL) characterization of the sample are presented in Sec. III. Time-resolved measurements are described in Sec. IV.

**II. SAMPLE AND EXPERIMENTAL SETUP**

The sample investigated in this work was grown by molecular beam epitaxy using the In-flush technique.<sup>8</sup> It contains a single layer of InAs QDs grown at 524 °C, deposited on a GaAs substrate covered by an 800-nm GaAs buffer layer. The sample was capped with a 100-nm GaAs top layer. The indium flush was applied to the QDs at 5 nm.

The samples were investigated in a  $\mu$ PL setup presented schematically in Fig. 1(b). All measurements were performed

at low temperature with the sample immersed in superfluid helium ( $T < 2$  K) inside an Oxford SpectroMag bath cryostat. The cryostat was equipped with superconducting coils producing magnetic field up to 7 T, either in a Faraday or a Voigt configuration. High spatial resolution was assured in the experiment by using a specially designed reflection-type microscope objective<sup>9</sup> immersed together with the sample inside the cryostat. The diameter of the laser spot on the sample surface was below 1  $\mu$ m. Three different lasers were employed to excite the sample: nonresonant CW Nd:YAG (532 nm) and LED laser (650 nm) and a quasiresonant femtosecond oscillator tuned at a central wavelength of 760 nm.

The photoluminescence was resolved using a 0.5-m diffraction spectrometer with a CCD camera and an avalanche photodiode (APD) for ultrafast single-photon detection. Two different time-resolved techniques were used. Measurements of radiative lifetime were carried out using a low-jitter APD (idQuantique id50). The overall temporal resolution in this measurement was up to 40 ps.

The other time-resolved technique used in our experiment was a single-photon correlation measurement. In this case two independent monochromators with high-efficiency Perkin-Elmer APDs were used. The monochromators were tuned to pass photons from a single excitonic transition, set independently for each spectrometer. The setup was arranged in Hanbury-Brown–Twiss<sup>10</sup> configuration with a 50/50 nonpolarizing beam splitter. Signals from the APDs were recorded using a multichannel picosecond event timer HydraHarp400. The timer was started by a photon detection in one APD and stopped by a photon detection in the other APD. A histogram of the events was built as a function of the time delay between the detection of the two photons. The total temporal resolution of the setup was estimated to be 1.1 ns. The accumulation time of a single correlation histogram was up to several hours, depending on the intensity of the investigated emission lines.

**III. PHOTOLUMINESCENCE RESULTS**

The PL spectrum from the investigated structure consists of the emission related to the GaAs barrier (1.49 eV), self-assembled QDs<sup>11</sup> (1.25–1.30 eV), and the emission related to the wetting layer (WL) (1.42–1.44 eV). The  $\mu$ PL spectrum in the energy range of the expected WL emission consists of a broad peak [Fig. 2(a)] with a well-resolved sharp line

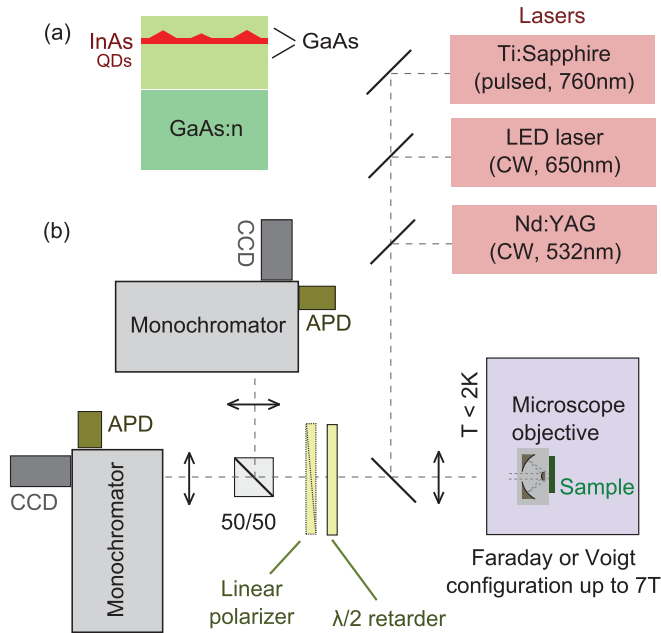


FIG. 1. (Color online) (a) Structure of the sample. (b) Schematic of experimental setup used in the study.

structure. This PL has been attributed to the recombination of electrons and heavy holes in the WL observed in similar QDs systems.<sup>12</sup> The structure of the peak shows that the WL is strongly disordered due to the composition and strain fluctuations. The disorder leads to potential fluctuations, which localize excitons. At some spots on the sample several well-resolved lines emerge in the spectrum at lower (by up to 10 meV) energies. We attribute these emission lines from the low-energy tail of the WL-related band as being related to the recombination of excitons in the WLQDs.

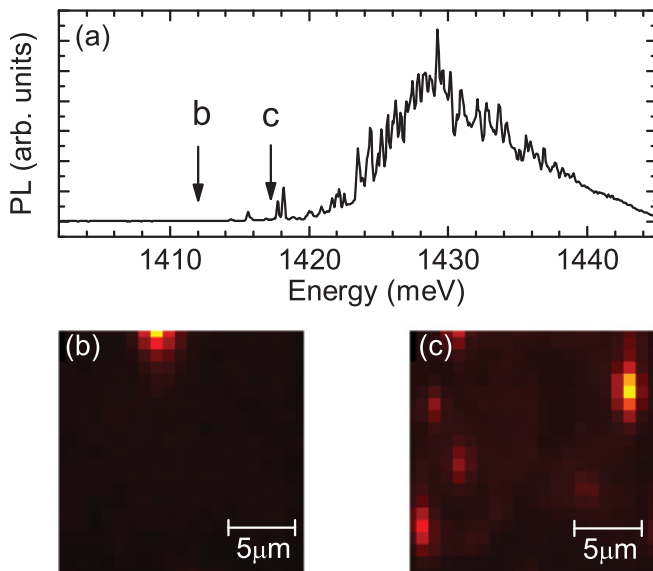


FIG. 2. (Color online) (a) The  $\mu$ PL spectrum from the structure with WLQDs. Spatial mapping of PL intensity monitored at (b) 1412 meV and (c) 1417 meV. The range of the presented maps was equal to  $20 \times 20 \mu\text{m}^2$

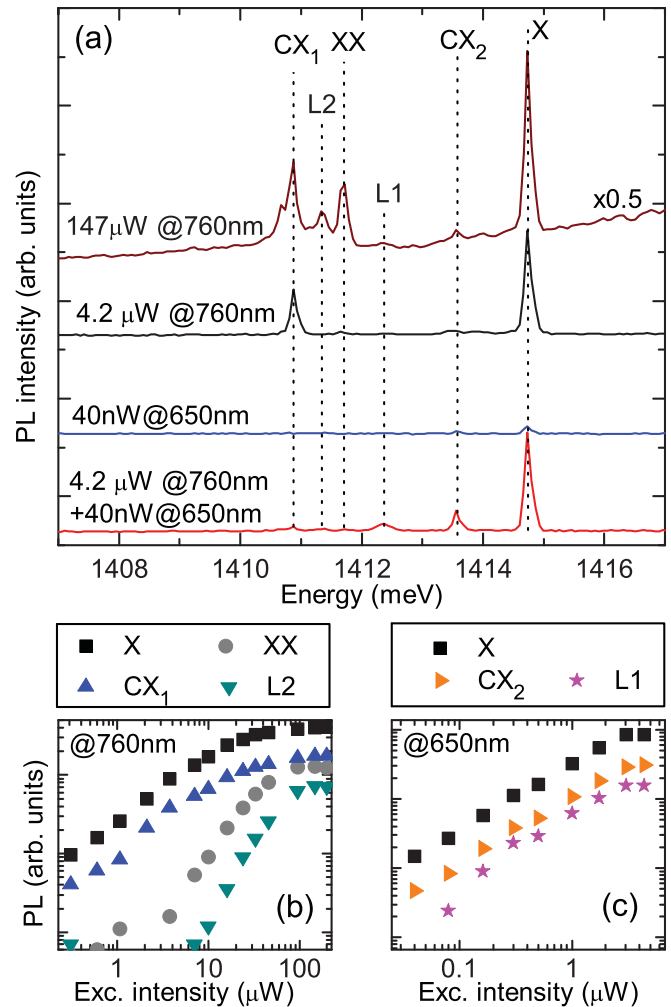


FIG. 3. (Color online) (a) PL spectrum of the same single QD under different excitation conditions. Dependence of the PL intensity on excitation power under excitation at (b) pulsed 760 nm and (c) CW 650 nm.

In order to provide more comprehensive characterization of the WLQD emission we analyzed PL properties of several different dots. All of them were characterized by relatively low emission energy, which was necessary to resolve the QD signal from the much stronger WL emission. We found that different dots shared the same PL pattern, including the same spectral order and similar spacing between various PL lines.

The typical spectrum of a single WLQD is presented in Fig. 3(a). Intensities of various PL lines present in the spectrum depend on parameters of excitation. With a weak-pulsed excitation (i.e., far from saturation of the QD emission) at 760 nm (1.63 eV) the PL spectrum features two main emission lines related to a neutral exciton (X) and charged-exciton ( $CX_1$ ) recombination. Under stronger excitation additional lines emerge: a line related to a neutral biexciton (XX) and a few other weaker lines, denoted for the sake of present study as L1 and L2. Detailed identification of these transitions is beyond the scope of the present study.

The identification of transitions X, XX,  $CX_1$ , and  $CX_2$  is firmly supported by measurements of polarization-resolved PL and magnetophotoluminescence. In the former case we

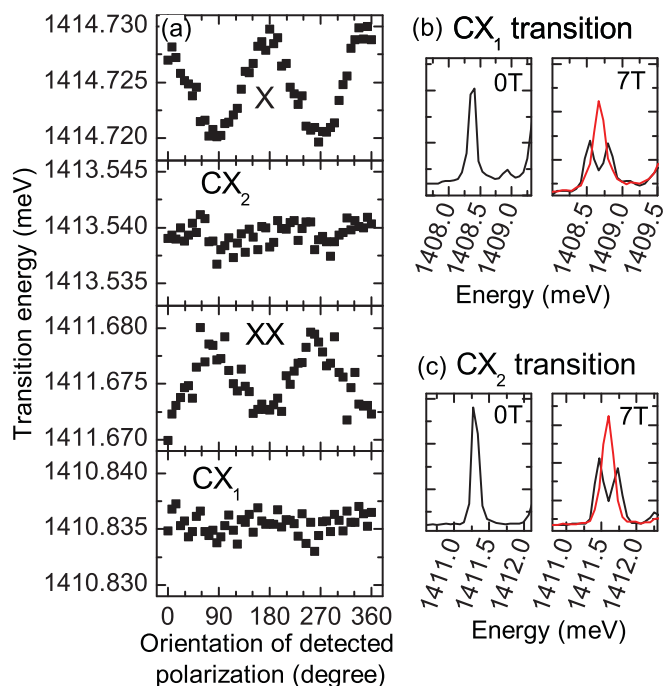


FIG. 4. (Color online) (a) Transition energies measured in selected linear polarization. Oscillatory behavior indicates small anisotropic splitting of about  $9 \mu\text{eV}$ . Splitting pattern of (b)  $\text{CX}_1$  and (c)  $\text{CX}_2$  transitions in magnetic field (Voigt configuration) measured for another dot. Black and red (gray) curves correspond to two perpendicular linear polarizations.

recorded PL spectra while changing the orientation of the detected linear polarization. By fitting Gaussian profiles to the analyzed spectral lines we extracted the apparent energies of each transition. The energies of the X and XX transitions exhibited clear sine-like oscillations [Fig. 4(a)], evidencing a splitting into two linearly polarized components<sup>13</sup> not resolved within our experimental resolution. The splitting is related to anisotropic exchange electron-hole interaction, which is characteristic of neutral excitons in QDs.<sup>14</sup> The splitting pattern allows us to attribute the X and XX emission lines to the neutral exciton and biexciton, respectively. The value of anisotropic splitting for the dot presented in Fig. 4(a) yielded  $9 \pm 2 \mu\text{eV}$ . The relatively low anisotropy of the neutral exciton is similar to the values found in natural QDs formed by interface fluctuations in thin quantum wells.<sup>14</sup>

Another important parameter of the excitation was the wavelength of the laser line. As we show in Fig. 3, WLQD emission can be strongly affected by this parameter, plausibly due to charge redistribution induced by higher-energy excitation, e.g., at 650 nm (1.91 eV). Data in Fig. 3 were obtained with relatively weak excitation of higher energy (100 times lower than simultaneous low-energy excitation), evidencing the sensitivity of the PL spectrum to the induced charge redistribution. The main observed change is the quenching of a charged-exciton line  $\text{CX}_1$  accompanied by the emergence of another line recognized as a charged exciton of the opposite sign  $\text{CX}_2$ .

No effect of in-plane anisotropy was detected for lines  $\text{CX}_1$  and  $\text{CX}_2$ , which confirms their attribution to charged excitons. Observation of both the neutral and the charged excitons is

usually reported in spectroscopic studies of nonresonantly excited QDs.<sup>15</sup> Further confirmation of the charged-exciton line identification was provided by measurements of PL in the magnetic field in the Voigt configuration [Figs. 4(b) and 4(c)]. In such a configuration, a splitting into four components is expected for charged-exciton transition as opposed to two bright components for the neutral exciton.<sup>16</sup> Our spectroscopic data confirm such a prediction for both  $\text{CX}_1$  and  $\text{CX}_2$  transitions [Figs. 4(b) and 4(c), respectively]. In both cases we observe symmetrical splitting into two pairs of lines linearly polarized along or perpendicularly to the field direction. The splitting of the inner doublet at 7 T is observable only as an increase in the linewidth, while the splitting of the outer doublet is more pronounced [ $0.29 \text{ meV}$  at 7 T as shown in Fig. 4(b) and  $0.27 \text{ meV}$  in the case of Fig. 4(c)].

#### IV. TIME-RESOLVED MEASUREMENTS

In order to verify the feasibility of using WLQDs as nonclassical light emitters we investigated the dynamical properties of WLQD PL by measurements of time-resolved photoluminescence and single-photon correlations.

The results of the measurements revealed subnanosecond lifetimes of the excitons confined in the WLQDs (Fig. 5). For single excitons we found lifetimes of  $0.57\text{--}0.85 \text{ ns}$  depending on the charge state. The neutral biexciton XX line exhibited a shorter lifetime of  $0.39 \text{ ns}$ . Measured lifetimes are 2 times shorter than the lifetime measured for an array of self-assembled InAs/GaAs QDs in the same sample, which yields about  $1.6 \text{ ns}$ .<sup>17</sup> The short lifetime of the WLQDs may be related to the weak lateral confinement.<sup>18</sup> Effective carrier recombination in the WLQDs may have important implications for the dynamics of carrier trapping in self-assembled QDs in

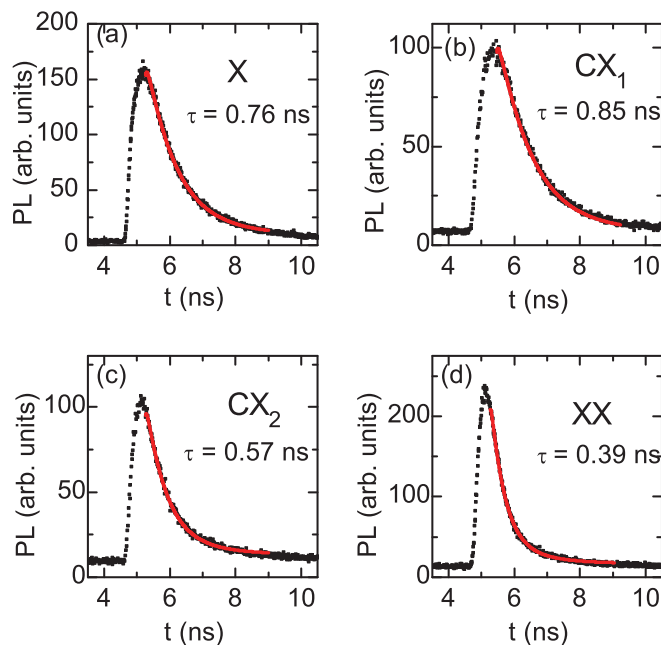


FIG. 5. (Color online) Time dependence of the PL signal for various lines of a single WLQD: (a) X line, (b)  $\text{CX}_1$  line, (c)  $\text{CX}_2$  line, and (d) XX line. Solid lines demonstrate fits of single exponential decays convolved with the response function of the detection setup.

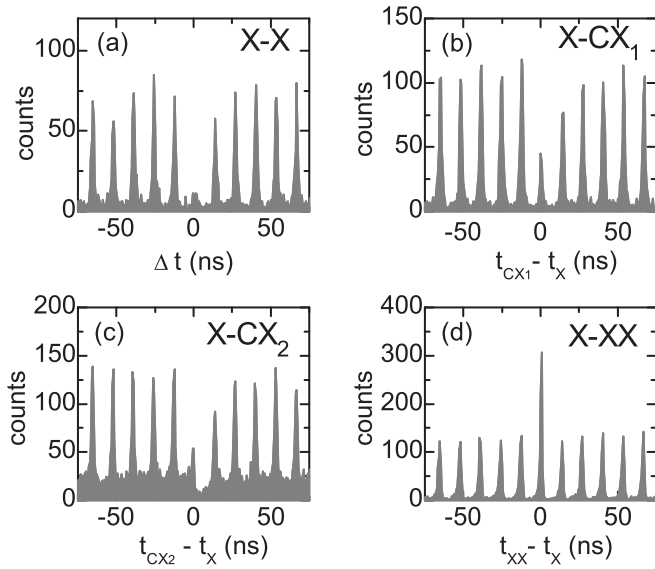


FIG. 6. Correlations between photons emitted from a single WLQD: (a) autocorrelation X-X, (b) cross-correlation X-CX<sub>1</sub> line, (c) cross correlation X-CX<sub>2</sub>, and (d) cross correlation X-XX. The cross correlation between the X and CX<sub>2</sub> lines was measured with additional weak CW illumination.

optoelectronic structures. Trapping electrons and holes in the WLQDs may influence lateral carrier transport in the WL.<sup>19–21</sup> A decreased efficiency of QD feeding with carriers may affect the performance of optoelectronic devices. Moreover, a possible in-plane energy transfer to lower-energy dots<sup>22</sup> would also have a detrimental effect on devices based on self-assembled dots due to uncontrolled reexcitation from the WLQD system.

The ultimate demonstration of the QD single-photon emission was provided by means of single-photon correlation measurements. Figure 6 presents a set of correlation results as histograms of the number of detected photon pairs of a given temporal separation. All measured histograms consist of distinct peaks separated by a laser repetition period of 13.2 ns. The width of each peak is governed by the relaxation time addressed in time-resolved PL measurements and the temporal resolution of the setup.

Autocorrelation of the X line shown in Fig. 6 exhibits well-pronounced suppression of a central ( $\Delta t = 0$ ) peak related to a photon antibunching effect. The relative height of the central peak amounted to a second-order correlation parameter of  $g^{(2)}(t=0) = 0.16 \pm 0.07$ . Comparison of the obtained  $g^{(2)}(t=0)$  parameter with its threshold value of 0.5 (Ref. 23) unequivocally proves the single-photon character of light emitted due to excitonic recombination in the studied WLQD. In the case of a perfect single-photon emitter, the  $g^{(2)}(t=0)$  value should read exactly 0. However, in the experiment the APD counts were related not only to the WLQD emission but also to spectrally broad PL background at the onset of the WL emission. The latter emission is characteristic of the ternary quantum wells and results from well width and alloy fluctuations and impurity-assisted processes.<sup>24</sup> We estimate the contribution of this excess signal to the  $g^{(2)}(t=0)$  in our experiment to be about 0.12, which is in agreement with the measured  $g^{(2)}(t=0)$  value. Due to different spectral

dependences of the WLQD emission and the background, this contribution can be further decreased by improving the spectral resolution of the setup down to the actual linewidth of the excitonic line. In particular, in the idealized case of lifetime-limited linewidth we would expect  $g^{(2)}(t=0)$  of the order of  $10^{-4}$ . This estimation needs to be accordingly increased if we include additional inhomogeneous broadening mechanisms.

We exploited two independent monochromators in the Hanbury-Brown–Twiss configuration to measure also cross-correlations between different lines of a single WLQD [Figs. 6(b)–6(d)]. Strong correlation evidenced as increase or decrease of the intensity of the central peak confirmed our previous attribution of PL lines to the same single WLQD.

Each cross-correlation histogram reflects the relation between correlated transitions. Specifically, in the case of cross correlations between neutral and charged excitons we observed an antibunching effect comparable to the X-X autocorrelation discussed previously. A faint asymmetry of a side peak height may be related to processes of a single-carrier capture;<sup>5</sup> however, low signal intensity did not allow us to elaborate on this effect.

An interesting effect was observed for X-CX<sub>2</sub> cross correlation [Fig. 6(c)], which was measured using weak above-barrier illumination to increase the intensity of the CX<sub>2</sub> line. The mixed excitation regime (pulsed excitation + CW illumination) was reflected in the correlation histogram, which featured both well-pronounced peaks at the laser repetition period and a recognizable CW background. The height of the peaks exhibited similar asymmetry to the one observed in case of X-CX<sub>1</sub> correlation and attributed to the single-carrier-capture mechanism.<sup>5</sup> A similar effect was observed also for the CW component of the correlation histogram. The photon count in the range between the central peak and the consecutive one was found to be much smaller than in the other sections of the histogram. The difference is easily interpreted in terms of the single-carrier mechanism invoked earlier. Directly after the recombination of the neutral exciton the dot is empty and the emission of the charged exciton requires capturing the three carriers. Such a process is unlikely to occur using only weak illumination. Conversely, the next laser pulse can excite the dot to the dark exciton state and thus increase the probability of the creation of a charged exciton by the illumination during the next interpulse period. The difference between these two scenarios (three-carrier vs one-carrier capture) accounts for the discussed effect in the correlation histogram.

Finally, we also demonstrated a cascade-type cross correlation between the XX and X lines, as shown in Fig. 6(d). In this case the central peak was more pronounced than the average peak by a factor of  $g^{(2)}(t=0) = 2.5 \pm 0.2$ . The obtained value corresponds well to the relatively strong excitation regime that was used in our experiment.

## V. SUMMARY

In conclusion, we have shown that the wetting layer quantum dots coexisting with self-assembled QDs can be used as a source of quantum light. We were able to determine the



basic properties of WLQD emission, including identification of all main PL lines. The results supporting the presented identification include PL experiments with the external magnetic field and polarization-resolved PL measurements. Fine-structure splitting of the excitonic transition was found in the range around  $10 \mu\text{eV}$  without any special processing of the sample.

We also successfully demonstrated a variety of single-photon correlations between emission lines of a single WLQD. Our results unequivocally prove that the observed emission lines originate from a single dot and further support their

identification by asymmetry of the cross-correlation histograms. Moreover, our demonstration of a biexciton-exciton cascade in this system opens the possibility to pursue entangled photon-pair generation from WLQDs by further reduction of their in-plane anisotropy.

#### ACKNOWLEDGMENTS

This work has been supported by Polish Funds for Science 2009–2011 and the Foundation for Polish Science.

\*Deceased.

†adam.babinski@fuw.edu.pl

<sup>1</sup>*Optics of Quantum Dots and Wires*, edited by G. W. Bryant and G. Solomon (Artech House, Boston, 2005).

<sup>2</sup>C. Santori, M. Pelton, G. Solomon, Y. Dale, and Y. Yamamoto, *Phys. Rev. Lett.* **86**, 1502 (2001).

<sup>3</sup>K. Sebald, P. Michler, T. Passow, D. Hommel, G. Bacher, and A. Forchel, *Appl. Phys. Lett.* **81**, 2920 (2002).

<sup>4</sup>C. Couteau, S. Moehl, F. Tinjod, J. M. Gérard, K. Kheng, H. Mariette, J. A. Gaj, R. Romestain, and J. P. Poizat, *Appl. Phys. Lett.* **85**, 6251 (2004).

<sup>5</sup>J. Suffczyński, T. Kazimierzczuk, M. Goryca, B. Piechal, A. Trajnerowicz, K. Kowalik, P. Kossacki, A. Golnik, K. P. Korona, M. Nawrocki, J. A. Gaj, and G. Karczewski, *Phys. Rev. B* **74**, 085319 (2006).

<sup>6</sup>J. Hours, S. Varoutsis, M. Gallart, J. Bloch, I. Robert-Philip, A. Cavanna, I. Abram, F. Laruelle, and J. M. Gérard, *Appl. Phys. Lett.* **82**, 2206 (2003).

<sup>7</sup>A. Babiński, J. Borysiuk, S. Kret, M. Czyż, A. Golnik, S. Raymond, and Z. R. Wasilewski, *Appl. Phys. Lett.* **92**, 171104 (2008).

<sup>8</sup>Z. R. Wasilewski, S. Fafard, and J. P. McCaffrey, *J. Cryst. Growth* **201-202**, 1131 (1999).

<sup>9</sup>J. Jasny, J. Sepiol, T. Irngartinger, M. Traber, A. Renn, and U. Wild, *Rev. Sci. Instrum.* **67**, 1425 (1996).

<sup>10</sup>R. Hanbury-Brown and R. Q. Twiss, *Nature (London)* **178**, 1046 (1956).

<sup>11</sup>A. Babinski, M. Potemski, S. Raymond, J. Lapointe, and Z. R. Wasilewski, *Phys. Rev. B* **74**, 155301 (2006).

<sup>12</sup>S. Sanguinetti, M. Henini, M. Grassi Alessi, M. Capizzi, P. Frigeri, and S. Franchi, *Phys. Rev. B* **60**, 8276 (1999).

<sup>13</sup>G. Bester, S. Nair, and A. Zunger, *Phys. Rev. B* **67**, 161306 (2003).

<sup>14</sup>D. Gammon, E. S. Snow, B. V. Shanabrook, D. S. Katzer, and D. Park, *Phys. Rev. Lett.* **76**, 3005 (1996).

<sup>15</sup>J. J. Finley, A. D. Ashmore, A. Lemaître, D. J. Mowbray, M. S. Skolnick, I. E. Itskevich, P. A. Maksym, M. Hopkinson, and T. F. Krauss, *Phys. Rev. B* **63**, 073307 (2001).

<sup>16</sup>M. Bayer, G. Ortner, O. Stern, A. Kuther, A. A. Gorbunov, A. Forchel, P. Hawrylak, S. Fafard, K. Hinzer, T. L. Reinecke, S. N. Walck, J. P. Reithmaier, F. Klopff, and F. Schäfer, *Phys. Rev. B* **65**, 195315 (2002).

<sup>17</sup>T. Auer (unpublished).

<sup>18</sup>J. Hours, P. Senellart, A. Cavanna, E. Peter, J. M. Gérard, and J. Bloch in *Physics of Semiconductors: 27th International Conference on the Physics of Semiconductors*, AIP Conf. Proc. No. 772 (AIP, New York, 2005), p. 771.

<sup>19</sup>R. Heitz, T. R. Ramachandran, A. Kalburge, Q. Xie, I. Mukhametzhanov, P. Chen, and A. Madhukar, *Phys. Rev. Lett.* **78**, 4071 (1997).

<sup>20</sup>C. Lobo, R. Leon, S. Marcinkevicius, W. Yang, P. C. Sercel, X. Z. Liao, J. Zou, and D. J. H. Cockayne, *Phys. Rev. B* **60**, 16647 (1999).

<sup>21</sup>E. S. Moskalenko, M. Larsson, W. V. Schoenfeld, P. M. Petroff, and P. O. Holtz, *Phys. Rev. B* **73**, 155336 (2006).

<sup>22</sup>T. Kazimierzczuk, J. Suffczynski, A. Golnik, J. A. Gaj, P. Kossacki, and P. Wojnar, *Phys. Rev. B* **79**, 153301 (2009).

<sup>23</sup>P. Michler, A. Kiraz, C. Becher, W. V. Schoenfeld, P. M. Petroff, L. Zhang, E. Hu, and A. Imamoglu, *Science* **290**, 2282 (2000).

<sup>24</sup>M. S. Skolnick, K. J. Nash, M. K. Saker, S. J. Bass, P. A. Claxton, and J. S. Roberts, *Appl. Phys. Lett.* **50**, 1885 (1987).